Spray-deposited Carbon Nanotube Networks as High-performing and Stable Temperature Sensors

Oliver Schoppe*, Felix Willgerodt*, Lin Chung Ping*, Erdem Basegmez*, Felix Brandenburg*, Katharina Melzer, Bernhard Fabel, and Paolo Lugli
**these authors contributed equally*

Institute for Nanoelectronics
Department of Electrical Engineering and Information Technology
Technical University Munich
Munich, Germany

***Abstract*— Carbon nanotubes are a promising new sensor material and have proven to be highly sensitive to various influences. In this study, temperature sensors using a thin film of single-walled carbon nanotubes as resistive sensing element are fabricated using a scalable spray deposition process. Different passivation methods – glass and poly-dimethylsiloxan (PDMS) – are compared with the aim of insulating the sensors from external effects such as light, gas and water, improving measurement quality. While only unpassivated and PDMS-passivated sensors show drifting of resistance over time, all sensors have a temperature-resistance hysteresis. Yet a high temperature coefficient of resistance of -0.4 %/K is achieved and hysteresis can be minimized and drifting eliminated using glass passivation. All passivation methods used allow for successful insulation without significant loss of sensitivity.**

Keywords: Carbon nanotube, SWCNT, temperature, sensor, passivation, encapsulation, hysteresis

I. INTRODUCTION

Carbon nanotubes (CNTs) were made popular by S.Iijima in 1991, who was the first to produce CNTs using an arc-discharge evaporation method [1]. Due to their extraordinary characteristics like great thermal conductivity, high tensile strength and unique electrical properties, CNTs have been the object of intensive scientific research ever since. Areas of application include electronics, flexible electronics, energy, optics, solid mechanics and sensor technology [2, 3].

CNTs are cylindrical molecules with a high aspect ratio, very small in diameter (down to around 1 nm) and lengths up to several centimeters [4]. They can be thought of as a honeycomb monolayer sheet of carbon (graphene) that is "rolled up", forming a seamless cylinder, a single-walled carbon nanotube (SWCNT). Since they can vary in diameter, there are also coaxial structures of several tubes, forming multi-walled carbon nanotubes (MWCNT) [5], which is depicted in Fig. 1.

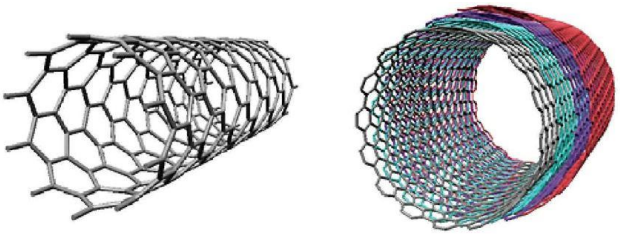

Fig. 1. The properties of carbon Nanotubes (CNTs) depend on their chirality and whether they are single-walled (left) or multi-walled (right).

The electrical properties of CNTs are greatly influenced by their topology, SWCNTs can be either semiconducting or metallic, depending on their chirality, while MWCNTs show mostly metallic conductivity [5-7] (although semiconducting MWCNTs have been reported by Zhuang et al. (2011) [8]). Semiconducting CNTs show very high electron mobility (around 10^5 cm²/Vs), exceeding all known conventional semiconductors and making them especially interesting for various applications like high speed transistors [9].

Due to their large surface-to-volume ratio, CNTs are very sensitive to outer influences, like binding of other molecules or temperature change. This can be used to build sensors, by measuring the change in electrical resistance in relation to those influences [3, 10]. However, the challenge in building an accurate sensor lies in isolating the desired parameter from all the other effects on the resistivity. The aim of this paper is to build CNT based temperature sensors and examine different passivation techniques, trying to eliminate all unwanted influences.

Previous studies on temperature sensors (using mostly dielectrophoretic assembly and passivation with a thin parylene layer) have shown good results with CNTs as sensor material, achieving good functionality and sensitivity [11, 12]. However, reduction of cross-sensitivities through passivation has not been assessed. In this study, multiple sensors are manufactured with an automated spraying process and passivated with PDMS or glass. The devices are evaluated in terms of temperature sensitivity and passivation effectiveness.

II. METHODS

A. Fabrication of CNT based Temperature Sensors

To investigate the idea to use CNTs as temperature sensors, different sensors were fabricated on a single wafer. All units consist of an interdigitated electrode structure (IDES) on which a thin film of single walled CNTs was deposited (see Fig. 2). The CNTs form a network, which serves as a temperature sensitive resistance between the electrodes. A total of 9 different sensors were manufactured to combine three different spacings between the interdigitated electrodes (100 µm, 200 µm, and 500 µm) with three different passivation techniques (no passivation: "naked", a layer of Polydimethylsiloxan (PDMS), glued on glass). This allows exploring the possibilities of passivating the sensors by comparing a bare CNT film ("naked"), which is fully exposed to any environmental influence, with two covered versions that insulate the sensors from external effects.

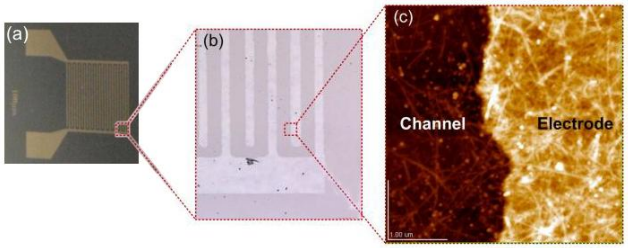

Fig. 2. a) Photo of one CNT-based temperature sensor on silicon wafer. b) Optical microscopy image of the IDES structure details (spacing of 100 µm). c) AFM image of a 4x4 µm² area showing parts of the Au electrode and the CNT network ("channel").[14]

A p-doped silicon substrate (500 µm thick) with a 200 nm SiO_2 surface was cleaned with acetone and propanol. The structure for the interdigitated electrodes was created in a layer of photoresist (ma-N-1420, Micro Resist Technology GmbH) on the silicon substrate using standard photolithography and a developer (ma-D 533s, Micro Resist Technology GmbH). The electrodes were produced by evaporating a 40 nm layer of gold on a 5 nm layer of chromium (for better adhesion) on the substrate. After lift-off of the remaining photoresist, chromium and gold, the wafer was treated with oxygen plasma (at 0.3 mbar for 1 min) and (3-Aminopropyl)triethoxysilane (APTES) to hydrophilize the surface. This step ensures the uniformity of the CNT film, which is deposited by spraying a 1:14 solution of CNTs and H_2O. The solution was produced by dispersing a powder of P3-SWCNTs (Carbon Solutions Inc.) with a carbonaceous purity over 90% and a metal content of 5-8 w% (weight percent, determined by thermal gravimetric analysis in air) in deionized water with carboxymethyl cellulose (CMC; as surfactant). An even CNT film distribution was achieved by using an automated spraying process as described by Abdellah et al. (2011) [13] and (2013) [14]. After deposition, the CMC was removed using diluted nitric acid (68% HNO_3 in H_2O). Although the thickness of the CNT film was not assessed, it can be estimated to be in the range of 10-20 nm if the sheet resistances (see Fig. 6) and the findings of Abdellah et al. (2011) [13] are taken into consideration.

For each IDES spacing, one sensor was left uncovered ("naked"), one sensor was passivated by applying a layer of PDMS (Dow Corning OS-20:Dow Corning 3522=1:10, cured at 100 °C for 5 min; about 2 mm thick) and one sensor was passivated by gluing a thin glass lid onto the IDES (glue: OP-4-20632 Dymax, cured with UV light for 15 min). Both passivation techniques ensured that the entire IDES was completely covered. While the PDMS was added in the presence of ambient air, the glass was glued on under a nitrogen atmosphere.

B. Experimental Setup for Sensor Evaluation

To evaluate the performance of the CNT network as a temperature sensor, a setup was used that allows the measurement of the resistance over time while controlling the temperature (see Fig. 3). The resistance of the CNT network between the fingers of the IDES was measured by a LCR meter (Agilent E4980A Precision; range from 0.1-1 mA at 10 kHz) using precision contact needles. The temperature was recorded with a PT100 on top of the substrate and controlled with a thermoelectric Peltier cooler underneath, which was driven by a Keithley 2602 System SourceMeter. The entire setup was driven by software (LabView).

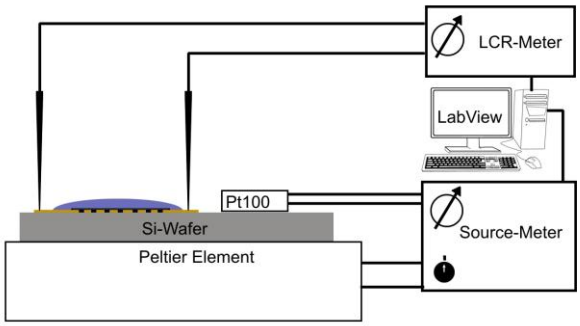

Fig. 3. A simplified schematic of the experimental setup (not to scale).

For analysis of thermoresistive and thermodynamic behavior, the temperature was varied from 25 °C to 45 °C and back in 10 cycles. Measurements were taken for cycle lengths of 50 s, 100 s and 200 s each. A typical variation of temperature over time can be seen in Fig. 4. During all measurements, the ambient temperature was between 24 °C and 25 °C and air humidity at 21%. To determine the effect of environmental influences for each passivation technique, the change of resistance at constant temperature (at 25 °C) was measured for the effect of light (690 lm white LED, 15 cm over sensor), air puffs (25 °C with air humidity of 21%; 3 consecutive puffs of 1 s duration; 1 bar through 5 mm nozzle in 5 cm distance), and water (distilled water from Nalgene at 25 °C). Furthermore, the measurement of the effect of light was repeated with an additional layer of aluminum foil on paper substrate on top of the sensors. Instead of a regular bulb, a LED was used to prevent a change in temperature on the sensor surface. The temperature of the air puffs and the deionized water was kept at 25 °C (just like the sensors itself) for the same reason. Hence, any change in resistance can clearly be attributed to the disturbance effect.

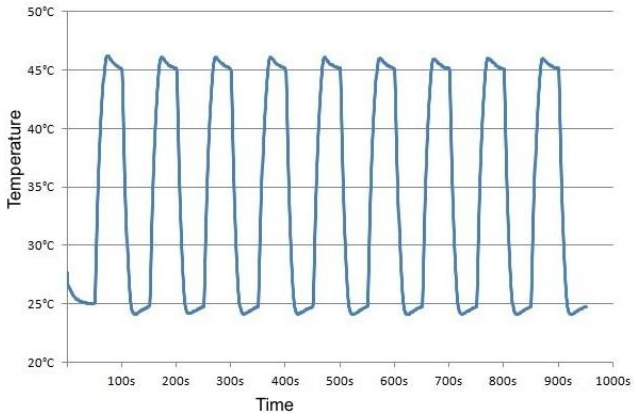

Fig. 4. Change in temperature over time for 10 cycles. Here, each cycle (from 25 °C to 45 °C and back) lasts 100 s.

III. Results and Discussion

A. Performance as a Temperature Sensor

A typical behavior of a CNT based thermal sensor is shown in Fig. 5. The temperature-resistance behavior is quite stable over multiple cycles and shows a significant change of electrical resistance in dependence of the temperature, which is desirable for the use as a temperature sensor. However, a hysteresis was observed for all 9 sensors: the resistance at T = 35 °C is constantly lower during the heating part of the cycle than during the cooling part (further discussion see section III. B). The temperature coefficient is negative (resistivity decreases with the increase of temperature) due to the fact that 90% of the CNTs used are of semiconducting nature.

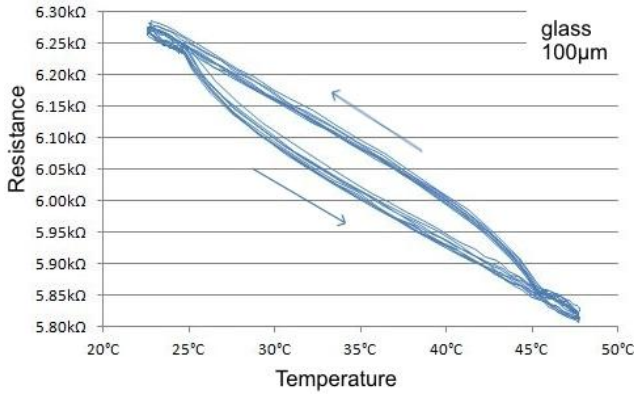

Fig. 5. A typical graph showing the resistance as a function of temperature reveals the negative temperature coefficient and the hysteresis effect. Here, a 100 µm glass-covered sensor was measured in cycles of 100 s duration.

The electrical resistances at 25 °C (defined as R_0) of the sensors are illustrated in Fig. 6. Naked and PDMS passivated sensors are in the range of a few thousand Ohms, while glass passivated sensors show resistances about eight times larger. The resistances for all sensors increase with the larger IDES spacings, as they are proportional to the distance the current has to flow through the CNT network. The relationship between IDES spacing and R_0 is linear.

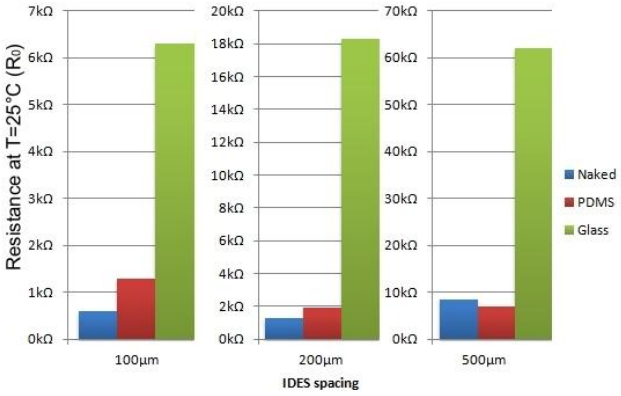

Fig. 6. The absolute resistance R_0 of all sensors was measured at T = 25 °C. The type of passivation and the IDES spacing determine R_0.

To determine the stability of resistance over time at a constant temperature, the resistance tolerance was calculated for all types of passivation. Resistance tolerance was calculated by determining resistance deviation as compared to the expected value E[R] during a period of 60 s for a constant temperature of T = 25 °C.

$$Resistance\ Tolerance = \frac{\int_{0s}^{60s} \sqrt{(R_{t=\tau} - E[R])^2}\, d\tau}{E[R] \cdot 60s}$$

The average resistance tolerance for each passivation is shown in Fig. 7. All sensors show a high stability with average deviations in the range of 0.01% to 0.03%. The naked sensors are slightly more stable than the others, which indicates that the passivation has a small effect on the resistance tolerance of the sensors.

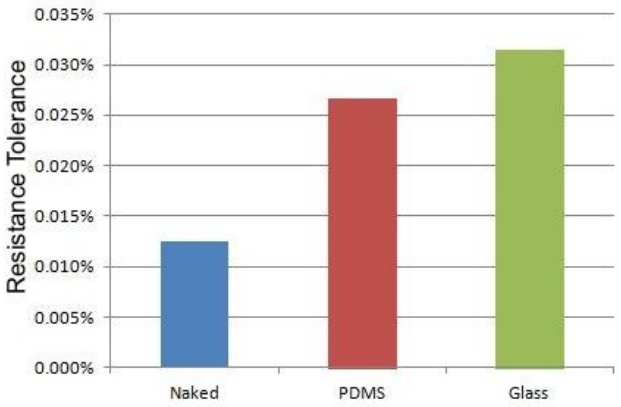

Fig. 7. The temporal stability of the resistance of the sensors is measured as the resistance tolerance. It is a metric for the deviation of resistance caused by noise at a given temperature of T = 25 °C.

To assess the functionality as a temperature sensor, the temperature coefficient of resistance (TCR) was used as a metric for the sensitivity. The TCR was calculated by following formula:

$$TCR = \frac{R_{T=45°C} - R_0}{R_0 \cdot 20K}$$

Fig. 8 shows the TCR for all 9 sensors (8a) and the average TCR per passivation (8b). First of all it is noteworthy that the resistance tolerance of any sensor is about ten times smaller than the change in resistance for a temperature change of 1K. Hence, given their stability and sensitivity, this type of CNT

based sensors is capable of reliably and precisely predicting temperature. The TCR values are negative due to the already mentioned negative temperature coefficient. While sensitivity varies among different IDES spacings, it does not seem to follow a specific trend (Fig. 8a).

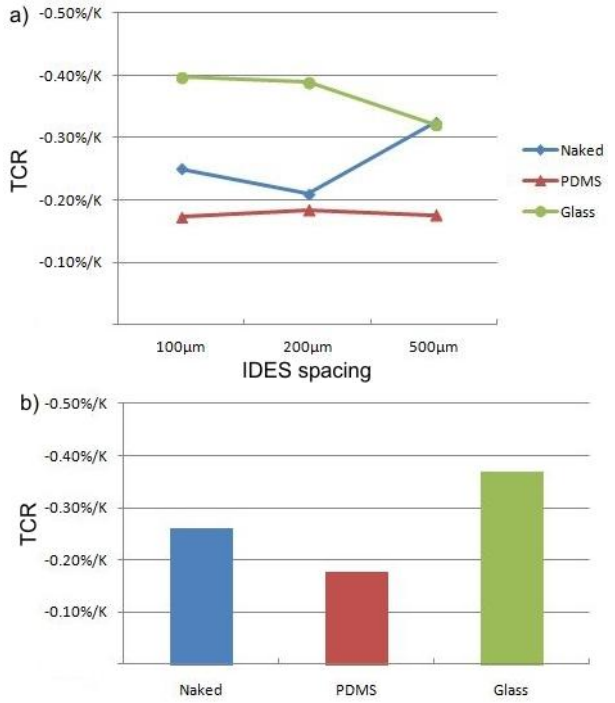

Fig. 8. The temperature coefficient of resistance (TCR) describes the relative change in resistance per 1K change in temperature. The individual TCRs can be seen in a), whereas b) shows the average TCR per passivation technique.

Fig. 8b shows that the average TCR of PDMS passivated sensors is lower than the one of naked sensors, yet the one of the glass configuration is higher. While the TCR values indicate high temperature sensitivity for all sensors, the glass passivation shows the best performance. This could be attributed to the fact that the glass was glued onto the sensor under an inert nitrogen atmosphere, while the PDMS was added under normal ambient conditions, resulting in a small amount of air trapped between the passivation material and the sensor. CNTs change their electrical behavior in the presence of certain molecules, like H_2O or O_2, also found in air [8]. Binding of such molecules to the CNTs results in a doping effect, ultimately influencing the temperature sensitivity. The glass configuration has no air trapped between sensor and passivation and insulates from ambient molecules and thus has the highest sensitivity. The TCR of the PDMS sensors could be lower because any doping molecules cannot be removed through thermal annealing like in naked sensors.

While the average TCR values of the nine sensors are slightly higher than values taken from literature, all are within the same range. A study with three dimensional SWCNT temperature sensors conducted by Selvarasah et al. (2007) [11] showed a TCR in the range of -0.157 %/K to -0.232 %/K. Fung and Li (2004) [12] passivated a MWCNT sensor with parylene C, resulting in a TCR in the range of -0.15 %/K to -0.18 %/K. Agarwal et al. (2008) [15] fabricated a CMOS integrated thermal sensor using SWCNTs and parylene C passivation, resulting in a TCR value of up to -0.40 %/K over a temperature range from 25 °C to 105 °C.

B. Temperature-Resistance Hysteresis and Drifting

Hysteresis behavior in the resistance-temperature relationship is observed for all passivations and all cycle durations. A drifting of the hysteresis curve can be seen for the naked and PDMS passivations for almost all IDES spacings and cycle lengths (Fig. 9), while all glass passivations have a relative stable hysteresis (Fig. 5) without drifting behavior. To compare the extent of the hysteresis effect between the different sensors, the relative hysteresis is calculated:

$$Relative\ Hysteresis = \frac{R_{T=35°C,Cooling} - R_{T=35°C,Heating}}{R_0}$$

Fig. 8 shows the dependency of the relative hysteresis on the duration of the temperature cycles for all sensors with an IDES spacing of 100 µm. The hysteresis effect seems to be the smallest when the temperature is changed relatively fast (entire cycle from 25 °C to 45 °C and back within 50 s) and tends to increase with longer cycle durations. However, for the glass passivated sensor, the peak in hysteresis was observed at a cycle duration of 100 s.

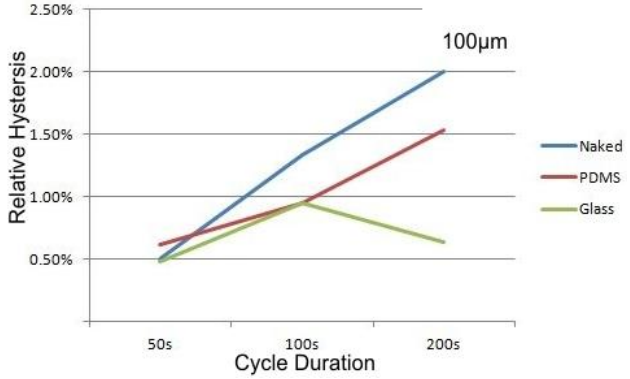

Fig. 9. The relative hysteresis shows a trend to increase with longer cycle durations.

While a temperature-resistance hysteresis for CNTs has been reported previously [16], no study has examined its cause in detail. However, hysteresis curves in current-voltage characteristics of CNTs have been observed in several studies. The cause of this hysteresis has been explained differently. According to Lee at al. (2007) [17], hysteresis is caused by charge traps which are a result of molecules binding to the CNTs. The charge transfer between the CNTs and charge traps at the siliconoxide/ambient air interface are presented as the main influence in Lee at al. (2007) [17], while Kim et al. (2003) [18] found that hysteresis phenomena correlate with water-siliconoxide surface chemistry, again resulting in charge traps. Related to this result, hysteresis was shown to increase with increasing humidity.

This could explain the differences between the passivation techniques. The naked configuration has a direct contact with ambient air, which could lead to a fairly large hysteresis. While both, PDMS and glass, prevent any ambient air to reach the CNT film, the hysteresis for those sensors might be explained by the same effect. The passivation of the sensors was not done in a vacuum, but in the presence of air. It is not unlikely that the sensors where passivated while having molecule such as oxygen or water bound to the CNTs.

The differences in hysteresis due to different cycle durations may be caused by the period of time water molecules need in order to bind to the surface. The shorter the

cycle, the less time the molecules have to bind to and detach from the CNTs, thus a smaller hysteresis.

The drifting effect that occurred for naked and PDMS sensors is shown in Fig. 10. Drifting could also be attributed to the binding of ambient molecules to the CNTs, as Fung and Li (2004) [12] found a significant decrease of drifting of their parylene C protected sensor after a thermal annealing cycle. This would be consistent with the observation that the drifting effect decreases with every cycle. Hence, the temperature cycles have a thermal annealing effect that stabilizes the sensor behavior.

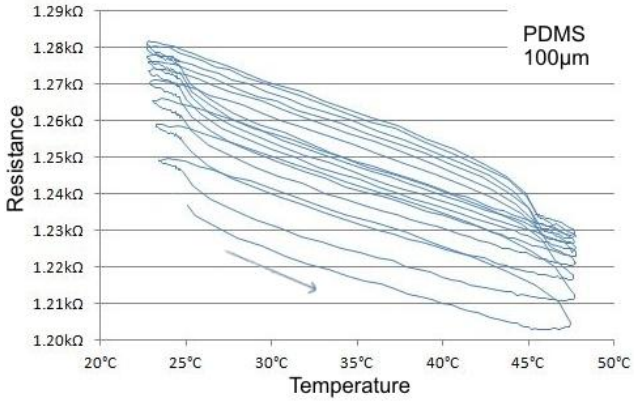

Fig. 10. Typical T-R-hysteresis for naked and PDMS encapsulated sensors shows a drifting effect that seems to stabilize after time (the drift between loops becomes smaller). Here, a 100 µm PDMS-covered sensor was measured in cycles of 100 s duration.

C. Disturbance Effects and Passivation

CNTs are very sensitive to several influences and therefore a CNT based thermal sensor ideally has to be insulated from unwanted influences in order to measure the temperature correctly. The different passivation techniques were evaluated by assessing the effects of light, air puffs and water drops on the resistance of the sensors at a constant temperature of 25 °C.

Fig. 11 shows the effect incident light (as described in section II B) on the resistivity of the sensors (IDES spacing of 100 µm). To observe any changes in resistance during and after illumination, the LED emits light only between t = 60 s and t = 120 s. During this period, the resistance decreases for all sensors by a small amount, showing that light has an influence on resistivity and has to be considered for the use of the sensors. Although all sensors show random changes in resistance in the range of the respective resistance tolerances at any given time, the shift in resistance during illumination is clearly visible. None of the passivation methods can shield the sensor successfully from this effect, yet the change in resistance for the used light source is rather small (under 0.5%). This could be explained by the photoconductive effect: photons with enough energy move an electron from the valence band to the conductance band, which increases the conductance of the CNTs [19]. However, the effect could also be explained by molecular photodesorption, as Chen et al. (2001) [20] observed in CNTs. For further confirmation, a light-blocking aluminum foil was placed on top of the passivated devices and the measurement was repeated. The data from this setup (not shown) revealed no significant change in resistance during illumination, supporting our primary assumption.

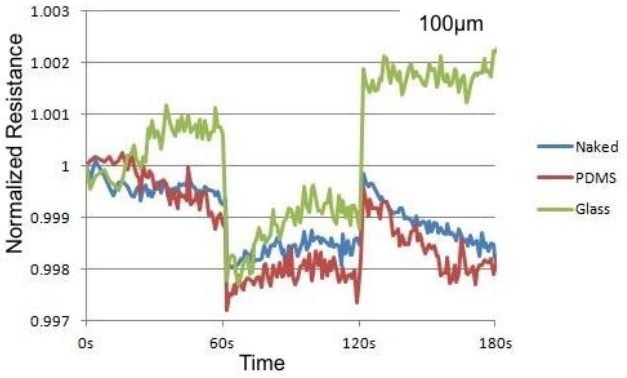

Fig. 11. Shining light onto the sensors (from t = 60 s until t = 120 s) shows a significant effect on the resistance. To compare the different passivations, the resistance over time was normalized to be 1 at t = 0 s.

The effect of air puffs on the resistance of sensors with an IDES spacing of 100 µm is shown in Fig. 12. As expected, passivated sensors do not show any change. However, for naked sensors the resistance immediately increases significantly and then slowly goes back to the initial value within a minute. As Jhi et al. (2000) [21] already stated, certain molecules can bind to the CNTs and thus can influence their resistance (see also Kong et al., 2000 [22]). Collins etc al. (2000) [23] found that especially oxygen tends to bind to the nanotubes surface, which cannot only change resistance significantly, but even change whether the TCR of a CNT network is positive or negative. It seems reasonable that the oxygen molecules which are already bound to the CNT are blown away by air puffs or replaced by other gases. Afterwards, the initial equilibrium state of molecules bound to the CNTs slowly recovers. This could explain the observed behavior for the naked sensors. Both passivations seem to be able to prevent this effect successfully, as no air puff can reach the sensor material.

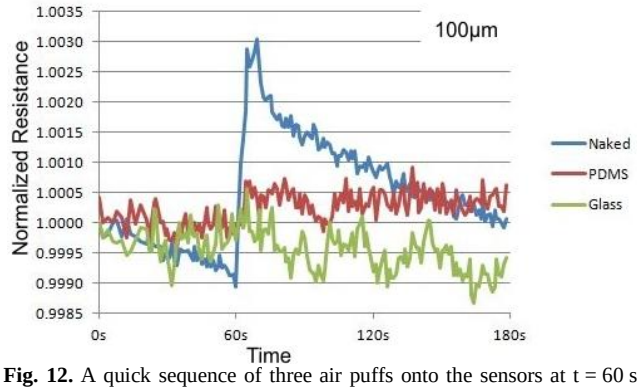

Fig. 12. A quick sequence of three air puffs onto the sensors at t = 60 s shows a small but significant increase in resistance for naked sensors. To compare the different passivations, the resistance over time was normalized to be 1 at t = 0 s.

The effect of pouring a drop of deionized water on the sensors (again, IDES spacing of 100 µm) is shown in Fig. 13. The naked sensor shows a big increase in resistance when exposed to water, which slowly decreases and then stabilizes at a high level of 145% of its initial resistance. This could be explained by chemical effects on the CNT surface. Water could cause two different types of charge traps which affect the resistance of the nanotubes. First, water molecules can be adsorbed to the CNTs surface [18].

Second, the SiO_2 surface could hydrate, which creates charge traps between the CNTs and this new surface [24]. Both would explain the dramatic change in resistance for naked sensors, which is not observed for passivated sensors, as the water cannot reach the CNTs. However, the glass covered sensor also showed a small but significant change in resistance, which was unexpected. It could either be caused by a small unintentional difference in temperature between the water and the sensors. Or it was caused by the mechanical impact of the water drop onto the glass above the CNTs that did not show in the thicker PDMS layer.

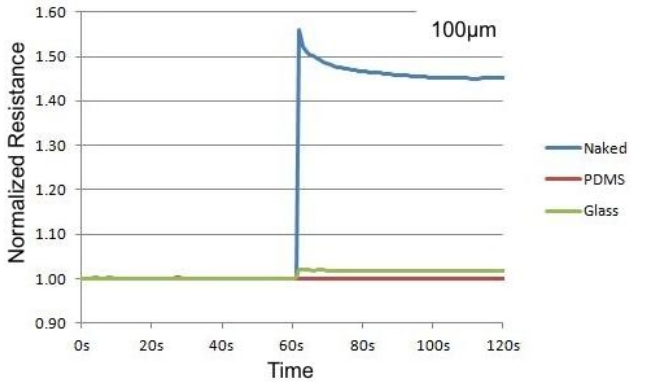

Fig. 13. A drop of deionized water onto the sensors at t = 60 s shows a significant increase in resistance for naked sensors. To compare the different passivations, the resistance over time was normalized to 1 at t = 0 s.

IV. Conclusion

In this study, SWCNT thin film temperature sensors were fabricated and evaluated with respect to stability, sensitivity and effectiveness of different passivation techniques. All sensors have a stable temperature-resistance behavior (resistance tolerance: 0.01% – 0.03%) and relatively high temperature sensitivity (TCR: -0.2 %/K – -0.4 %/K). While all sensors show a temperature-resistance hysteresis, only naked and PDMS-passivated ones also have a drifting effect that seems to vanish after thermal annealing cycles.

Both passivation techniques (PDMS and glass) seem generally capable to insulate the sensors from disturbing effects such as interaction with gas molecules and water. Passivation from visible light can easily be achieved by adding thin aluminum foil on top of the passivation layer. In conclusion, the glass passivation technique seems to be superior to PDMS, as it tends to lead to greater sensitivity, shows the smallest relative hysteresis and does not need thermal annealing cycles for stable behavior (no drifting). Yet, applying the PDMS passivation under an inert Nitrogen atmosphere might help reduce hysteresis and drifting and increase sensitivity.

Further research is needed to assess the causes, the precise characteristics and the consequences of the observed hysteresis effect. While oxygen and water are believed to be the main cause of this behavior, more detailed knowledge of intrinsic CNT behavior and the effects of oxidation and hydration would be helpful for fabrication of hysteresis-free temperature sensors with random CNT networks.

References

1. S. Iijima (1991). Helical Microtubules of graphitic carbon. Nature 354: 56-58
2. M. Endo , M. Strano, and P. Ajayan (2008). Potential Applications of Carbon Nanotubes. Topics in Applied Physics, 111:13-61
3. L. Hu, D. Hecht, and G. Grüner (2010). Carbon Nanotube Thin Films: Fabrication, Properties, and Applications. Chemical Review, 110: 5790–44
4. X. Wang, Q. Li, J. Xie, Z. Jin, J. Wang, Y. Li, K. Jiang, and S. Fan (2009). Fabrication of ultralong and electrically uniform single-walled Carbon nanotubes on clean substrates. Nano Letters, 9:3137-41
5. H. Wong and D. Akinwande (2010). Carbon nanotube and graphene device physics. Cambridge University Press, Cambridge, UK
6. T. Odom, J. Huang, P. Kim, and C. Lieber (1998). Atomic structure and electronic properties of single-walled carbon nanotubes. Letters to Nature, 391:6662-64
7. R. Saito, M. Fujita, G. Dresselhaus, and M. Dresselhaus (1992). Electronic structure of graphene tubules based on C60. Physical Review B, 46:1804–11
8. R. Zhuang, T. Doan, J. Liu, J. Zhang, S. Gao, and E. Mäder (2011). Multi-functional multi-walled carbon nanotube-jute fibres and composites. Carbon, 49:2683-92
9. T. Durkop, S. Getty, E. Cobas, and M. Fuhrer (2004). Extraordinary Mobility in Semiconducting Carbon Nanotubes. Nano Letters, 4:35-39
10. M. Lucci, P. Regoliosi, A. Reale, A. Di Carlo, S. Orlanducci, E. Tamburri, M. Terranova, P. Lugli, C. Di Natale, A. D'Amico, R. Paolesse (2005). Gas sensing using single wall carbon nanotubes ordered with dielectrophoresis. Sensors and Actuators B, 111:181-186
11. S. Selvarasah, C. Chen, S. Chao, P. Makaram, A. Busnaina, and M. Dokmeci (2007). A Three Dimensional Thermal Sensor Based on Single-Walled Carbon Nanotubes. Solid-State Sensors, Actuators and Microsystems Conference, 1023-26
12. C. Fung and W. Li (2004). Ultra-low-power Polymer Thin Film Encapsulated CarbonNanotube Thermal Sensors. 4th IEEE Conference on Nanotechnology, 158-160
13. A. Abdellah, A. Yaqub, C. Ferrari, B. Fabel, P. Lugli, and G. Scarpa (2011). Spray Deposition of Highly Uniform CNT Films and Their Application in Gas Sensing. 11th IEEE International Conference on Nanotechnology, 1118-23
14. A. Abdellah, A. Abdelhalim, M. Horn, G. Scarpa, P. Lugli (2013). Scalable Spray Deposition Process for High Performance Carbon Nanotube Gas Sensors. IEEE Transaction on Nanotechnology, 1
15. V. Agarwal, C. Chen, M. Dokmeci, S. Sonkusale (2008). A CMOS Integrated Thermal Sensor Based on Single-Walled Carbon Nanotubes. Proceedings of IEEE Sensors Conference, 750-751
16. K. Karimov, M. Chani, and F. Khalid (2011). Carbon nanotube film based temperature sensors. Physica E, 43:1701-03
17. J. Lee, S. Ryu, K. Yoo, I. Choi, W. Yun, J. Kim (2007). Origin of Gate Hysteresis in Carbon Nanotube Field-Effect Transistors. The Journal of Physical Chemistry Letters, 111:12504-07
18. W. Kim, A. Javey, O. Vermesh, Q. Wang, Y. Li, and H. Dai (2003) Hysteresis Caused by Water Molecules in Carbon Nanotube Field-Effect Transistors. Nano Letters, 3:193-198
19. A. Fujiwara, Y. Matsuoka, H. Suematsu, N. Ogawa, K. Miyano, H. Kataura, Y. Maniwa, S. Suzuki, and Y. Achiba (2001). Photo-conductivity in Semiconducting Single-Walled Carbon Nanotubes. Japanese Journal of Applied Physics, 40:1229-31

20. R. Chen, N. Franklin, J. Kong, J. Cao, T. Tombler, Y. Zhang, H. Dai (2001). Molecular photodesorption from single-walled carbon nanotubes. Applied Physics Letters, 79: 2258-60

21. S. Jhi, S. Louie, and M. Cohen (2000). Electronic Properties of Oxidized Carbon Nanotubes. Physical Review Letters, 85:1710-13

22. J. Kong, N. Franklin, C. Zhou, M. Chapline, S. Peng, K. Cho, H. Dai (2000). Nanotube molecular wires as chemical sensors. Science, 287: 622-625

23. P. Collins, K. Bradley, M. Ishigami, and A. Zettl (2000). Extreme oxygen sensitivity of electronic properties of carbon nanotubes. Science, 287: 1801-04

24. L. Zhuravlev (2000). The surface chemistry of amorphous silica. Zhuravlev model. Colloids and Surfaces A, 173:1-38